Fluid Flow through Randomly Packed Columns and Fluidized Beds

The ratio of pressure gradient to superficial fluid velocity in packed columns is shown to be a linear function of fluid mass flow rate. The constants of the linear relation involve particle specific surface, fractional void volume, and fluid viscosity. These constants can be used to predict the degree of bed expansion with increasing gas flow after the pressure gradient reaches the buoyant weight of solids per unit volume of the bed. Formal equations are developed that permit estimation of gas flow rates corresponding to incidence of turbulent or two-phase fluidization—a state of flow in which gas bubbles, with entrained solids, rise through the bed and cause intense circulation of solids. A constant product of gas viscosity times superficial velocity may serve as a criterion of a standard state in fluidized systems used for reaction kinetic studies.

SABRI ERGUN AND A. A. ORNING

COAL RESEARCH LABORATORY AND DEPARTMENT OF CHEMICAL ENGINEERING, CARNEGIE INSTITUTE OF TECHNOLOGY, PITTSBURGH, PA.

THE use of fluidized beds for kinetic studies of heterogeneous reactions offers advantages in ease of temperature control even for highly exothermic reactions. However, it is essential to know the gas velocities needed to produce fluidization, and interpretation of data requires either a standard state of fluidization or some basis of correction for changes in bed volume and for nonuniformity of contact between gases and solids. This has required a study of the laws of fluid flow and new experimental data to describe the conditions of gas flow for rates ranging continuously from zero through those needed for fluidization.

If the behavior of a packed bed is followed when a gas stream is introduced from the bottom, the pressure drop at first increases with flow rate without bed expansion—i.e., the fractional void volume remains unchanged. When the flow rate is sufficient to cause a pressure gradient equal to the buoyant weight of the solids per unit volume, further increase in flow rate causes the bed to expand—i.e., increases the fractional void volume—the pressure drop remaining substantially constant. Up to a certain gas flow rate the expansion does not involve channeling or bubble flow, provided the column is subjected to some vibration. In this region the bed increasingly acquires fluid properties, ceases to maintain its normal angle of repose, and can be said to be partially fluidized. Until the gas flow rate is sufficient to cause bubble flow, there is no gross circulation or mixing of solids.

With increasing gas flow rates bubbles appear and the bed becomes fully fluidized—i.e., it can no longer maintain an angle of repose greater than zero—there is no resistance to penetration by a solid except buoyancy, and the solids are circulating or mixing. Continued increase in flow rate causes passage of larger bubbles with increasing frequency. This fluidized bed is not homogeneous with regard to concentration of solids. For this reason, it can appropriately be described as two-phase fluidization. Within the fluidized bed a denser but expanded bed constitutes the continuous phase, while bubbles, which probably contain solids in suspension, constitute the discontinuous phase. The relative proportion of these phases varies with flow rate.

The three distinctly different states—the fixed bed, the expanded bed, and the fluidized bed—are considered separately in that order.

THE FIXED BED

The fixed bed is identical with randomly packed beds involved in the determination of the specific surface of fine powders by the air permeability method (*1*, *6–8*, *10–13*) and with randomly packed columns (*3*, *5*, *9*, *15*, *18–20*) as used in absorption, extraction, distillation, or catalytic reactions.

Attempts to determine the specific surface of powders by the air permeability method have led to a considerable amount of work in connection with the pressure drop through fine powders and filter beds at low flow rates. The following equation, based upon viscosity, was first developed by Kozeny (*13*), proposed by Carman (*8*) for use with liquids, and later extended by Lea and Nurse (*14*) to include measurements with gases:

$$S_v = \left(\frac{1}{5}\frac{\Delta P}{\mu u}\frac{1}{L}\frac{\epsilon^3}{(1-\epsilon)^2}\right)^{1/2} \qquad (1)$$

It has been found satisfactory for small particles having specific surfaces less than 1000 to 2000 sq. cm. per gram. Arnell (*1*) and others have modified it to include terms which account for the changing flow characteristics in extremely fine spaces, a modification that is not of particular interest for the present purpose.

On the other hand, a considerable amount of work has been done in correlating data for packed columns at higher fluid velocities where the pressure drop appears to vary with some power of the velocity, the exponent ranging between 1 and 2. Blake (*3*) suggested that this change of relationship between pressure drop and velocity is entirely analogous to that which occurs in ordinary pipes and proposed a friction factor plot similar to that of Stanton and Pannell (*20*). The equation used was that for kinetic effect modified by a friction factor which in turn is a function of Reynolds number (*9*).

$$\Delta P = 2f\rho_f u^2/D_p \qquad (2)$$

where

$$f = \phi(N_{Re})$$

Recent workers (*7*, *15*) have included the effect of void fraction by the addition of another factor in Equation 2. It is usually given in the form $(1-\epsilon)^m/\epsilon^3$ where m is either 1 or 2.

A study of these different procedures showed that for fluid flow at low velocities through fine powders, viscous forces account for the pressure drop within the accuracy of measurement, whereas for higher velocities, kinetic effects become more important but do not alone account for the pressure drop without the aid of factors which in turn are functions of flow rate.

This transition from the dominance of viscous to kinetic effects, for most packed systems, is smooth, indicating that there should be a continuous function relating pressure drop to flow rate. A

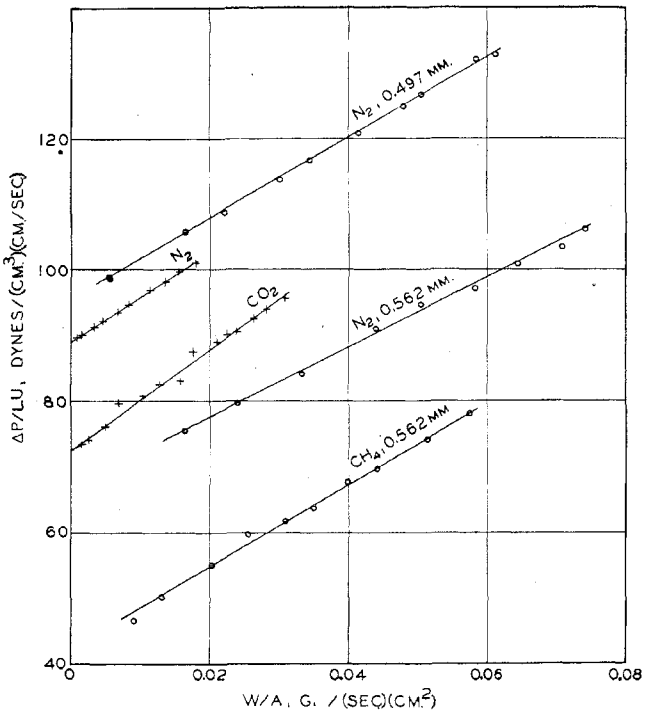

Figure 1. Permeability of Beds of Glass and Lead Spheres

Material	Gas	Av. Diam. of Spheres, Mm.	Fractional Void Volume
+ Glass	N_2	0.570	0.330
	CO_2	0.570	0.330
● Lead	N_2	0.562	0.362
	CH_4	0.562	0.352
	N_2	0.497	0.350

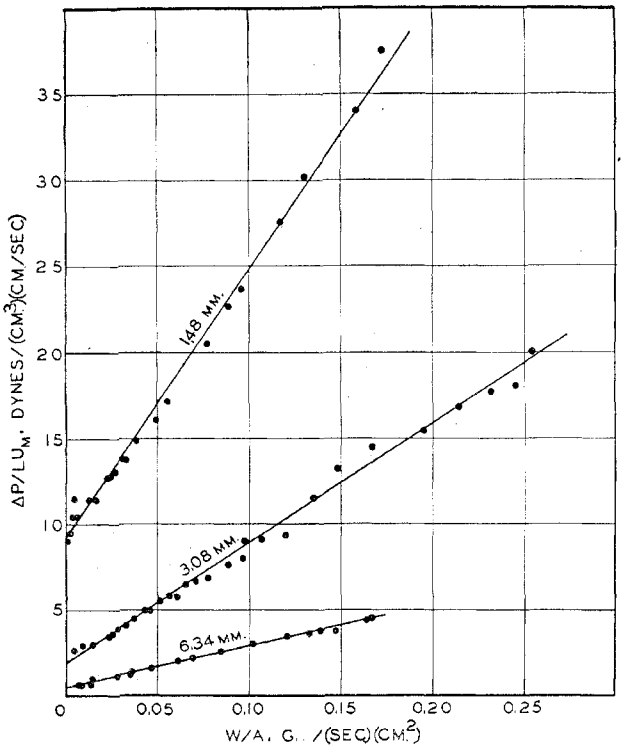

Figure 2. Air Permeability of Lead Shot

(Data of Burke and Plummer, 5)

Av. Diam. of Spheres, Mm.	Fractional Void Volume
6.34	0.397
3.08	0.383
1.48	0.375

general relationship may be developed, using the Kozeny assumption that the granular bed is equivalent to a group of parallel and equal-sized channels, such that the total internal surface and the free internal volume are equal to the total packing surface and the void volume, respectively, of the randomly packed bed. The pressure drop through a channel is given by the Poiseuille equation:

$$dP/dL = 32\,\mu u^*/D_c^2 \qquad (3)$$

to which a term representing kinetic energy loss, analogous to that introduced by Brillouin (4) for capillary flow, may be added.

$$dP/dL = 32\,\mu u^*/D_c^2 + {}^1/_2\,\rho_f u^{*2}/D_c \qquad (4)$$

Using relationships for cylindrical channels, the number of channels per unit area and their size can be eliminated in favor of specific surface and the fractional void volume by means of the following equations:

$$S_v = NL\pi D_c/L\pi(D^2/4)(1-\epsilon)$$

$$N\pi D_c^2/4 = \pi D^2\,\epsilon/4$$

$$u^* = u/\epsilon$$

and

$$D_c = \frac{4\epsilon}{1-\epsilon}\,\frac{1}{S_v}$$

This leads to:

$$dP/dL = 2\,\frac{(1-\epsilon)^2}{\epsilon^3}\,\mu u\,S_v^2 + \frac{1}{8}\,\frac{1-\epsilon}{\epsilon^3}\,\rho_f u^2 S_v \qquad (5)$$

This equation, like many others that relate pressure drop to polynomials of the fluid flow rate, differs from them in that the coefficients have definite theoretical significance.

For a packed bed, the flow path is sinuous and the stream lines frequently converge and diverge. The kinetic losses, which occur only once for the capillary, occur with a frequency that is statistically related to the number of particles per unit length. For these reasons, a correction factor must be applied to each term. These factors may be designated as α and β.

$$dP/dL = 2\alpha\,\frac{(1-\epsilon)^2}{\epsilon^3}\,\mu S_v^2\,u + \frac{\beta}{8}\,\frac{1-\epsilon}{\epsilon^3}\,\rho_f u^2 S_v \qquad (6)$$

The values for α and β can be determined experimentally and α generally approximates $(\pi/2)^2$ which has been proposed on theoretical grounds (12). Experiments with randomly packed materials of known specific surface have led to adoption of a value of 5 for 2α, which is close to the theoretical value of 4.935.

Integration of Equation 6, assuming isothermal expansion of an ideal gas, leads to the equation:

$$\Delta P/Lu_m = \frac{(1-\epsilon)^2}{\epsilon^3}\,2\alpha\mu S_v^2 + \frac{1-\epsilon}{\epsilon^3}\,\frac{\beta}{8}\,(W/A)S_v \qquad (7)$$

where u_m is the superficial velocity at the mean pressure, and W/A is the mass flow rate per unit area of the empty tube. Leva *et al.* (15) reported that in packed tubes, when the viscous forces are predominant, the pressure drop is proportional to $(1-\epsilon)^2/\epsilon^3$; whereas, at higher flow rates, the corresponding dependence upon the void fraction is $(1-\epsilon)/\epsilon^3$ which is just what would be expected from Equation 7.

From Equation 7, a plot of $\Delta P/Lu_m$ *vs.* W/A would give a straight line, the intercept and slope leading to values of α and β. Typical plots of data obtained to test this dependence of pressure drop on gas flow rate are shown in Figure 1.

Pressure drop measurements were made in a glass tube, 1 inch in inside diameter and 30 inches long, fitted with a fritted-glass disk to obtain uniform gas flow at the bottom and with pressure

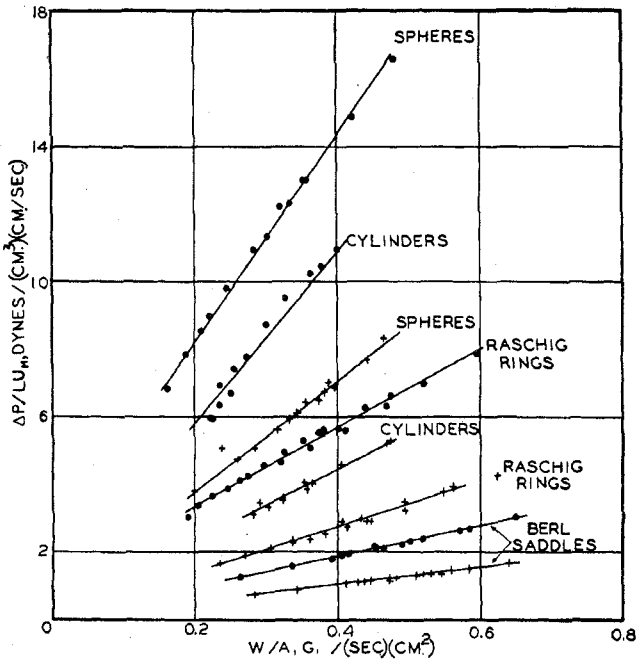

Figure 3. Air Permeability of Various Materials

(Data of Oman and Watson, *19*)

Material	Av. Diam. of Spheres, Inch	Fractional Void Volume (Approximate)
● Celite spheres	0.25	0.38
+ Celite spheres	0.25	0.46
● Celite cylinders	0.25	0.36
+ Celite cylinders	0.25	0.46
● Raschig rings	0.375	0.55
+ Raschig rings	0.375	0.62
● Berl saddles	0.5	0.71
+ Berl saddles	0.5	0.76

taps at the top and at a point just above the fritted-glass disk. Gas flow was measured with a series of capillary flowmeters, each calibrated against wet-test meters. Reproducible results in this small glass tube were most easily obtained if the size range of material in the bed was not too great and if the bed was thoroughly mixed by full fluidization before packing to the desired density. Excessive packing generally disturbed the incidence and uniformity of expansion. A brief summary of the conditions for which experimental data were obtained is as follows: particle size, 0.2 to 1.0 mm.; particle density, 1.5, 2.5, 7.8, 8.6, and 10.8 grams per cc.; particle shape, spherical and pulverized; gases employed, hydrogen, methane, nitrogen, and carbon dioxide; gas velocities, up to 100 cm. per second.

Figures 2 and 3 show data taken from the literature for experiments with air flowing through beds of lead shot 1.5 to 6.5 mm. in diameter (*5*) and Celite spheres, Celite cylinders, Raschig rings, and Berl saddles, each ranging from 0.25 to 0.75 inch in nominal size (*19*). These plots demonstrate the validity of Equation 7 within the range of experimental accuracy. Values for α and β for all the data are given in Table I, together with references to sources of those data taken from the literature. The lines shown in Figure 3 for the data of Oman and Watson (*19*) are not those used in determining the constants. These data fell into high and low density groups each of nearly, but not quite, the same fractional void volume. For these data, Equation 7 was first divided by $(1 - \epsilon)^2/\epsilon^3$, leading to plots with common intercepts convenient for determining α. Similarly, a division by $(1 - \epsilon)/\epsilon^3$ led to plots with common slopes for determining β.

Using the relation for a sphere, $D_p = 6/S_v$, Reynolds number, $N_{Re} = D_p U_m \rho_{fm}/\mu$, can be used to transform Equation 7 to the form

$$\Delta P/L = \left[1 + 96\,\frac{\alpha}{\beta}\,\frac{1-\epsilon}{N_{Re}}\right]\frac{\beta}{8}\,\frac{1-\epsilon}{\epsilon^3}\,S_v\rho_{f_m}u_m^2 \qquad (8)$$

Thus the friction factor would become:

$$f = a\left[1 + 96\,\frac{\alpha}{\beta}\,\frac{1-\epsilon}{N_{Re}}\right] \qquad (9)$$

An examination of the values of α and β given in Table I and of Equation 8 indicates the relative importance of the viscosity and kinetic terms. For Reynolds numbers around 60, with $\epsilon = 0.35$, the two have nearly equal effects upon pressure drop. For $N_{Re} = 0.1$, viscosity accounts for 99.8%, while for $N_{Re} = 3000$, kinetic effects account for 97% of the pressure drop. Because packed columns are generally operated in the range from $N_{Re} = 1$ to 10,000, both terms are essential in calculations of pressure drop.

Although the theoretical development has been based on randomly packed beds, the same treatment can be applied to data obtained (*2*, *17*) for geometrically arranged packings. In these cases the coefficients may differ markedly for different arrangements even at the same fractional void volume.

Table I. Coefficients for Pressure Drop Equation

Material	Fluid	Specific Surface, Cm.$^{-1}$	Sample Weight, Grams	Void Fraction	α	β	Source
Pulverized coke	Different gases	60-370	..	0.52-0.64	2.5	2.3	..
Glass beads	Hydrogen	264.0	200	0.343	1.9	3.0	..
	Carbon dioxide	105.2	200	0.330	1.8	3.1	..
	Nitrogen	105.2	200	0.330	1.9	2.8	..
Iron shot	Nitrogen	127.2	300	0.375	2.0	2.5	..
	Nitrogen	127.2	200	0.375	2.0	2.6	..
	Carbon dioxide	127.2	300	0.375	1.8	2.5	..
	Nitrogen	78.0	200	0.371	2.0	2.7	..
Lead shot	Nitrogen	120.7	500	0.350	1.9	2.7	..
	Carbon dioxide	120.7	500	0.350	1.8	3.1	..
	Nitrogen	106.8	300	0.352	1.8	2.7	..
	Methane	106.8	300	0.352	1.8	3.1	..
Lead shot	Nitrogen	75.2	1000	0.364	1.9	3.3	..
	Nitrogen	75.2	300	0.364	1.9	3.3	..
	Nitrogen	59.75	500	0.366	1.8	2.9	..
Copper shot	Carbon dioxide	90.0	500	0.372	1.8	2.6	..
Lead shot	Water	Different sizes	..	0.380	2.5	2.6	(*16*)
Lead shot	Air	40.6	..	0.375	2.0	2.6	(*5*)
	Air	19.5	..	0.383	2.3	2.5	(*5*)
	Air	19.5	..	0.390	2.2	2.5	(*5*)
	Air	9.57	..	0.421	2.8	2.0	(*5*)
Lead shot	Air	9.57	..	0.397	2.8	2.1	(*5*)
	Air	27.5	..	0.303	1.9	1.8	(*5*)
	Air	22.2	..	0.325	2.5	2.3	(*5*)
	Air	19.8	..	0.320	3.0	2.8	(*5*)
Spheres, Celite	Air	11.5	..	0.378	5.8	2.0	(*19*)
	Air	11.5	..	0.466	5.8	2.2	(*19*)
Cylinders, Celite	Air	8.78	..	0.365	5.7	1.7	(*19*)
	Air	8.78	..	0.457	4.9	1.6	(*19*)
Berl saddles, clay	Air	11.55	..	0.713	6.6	5.2	(*19*)
	Air	11.84	..	0.764	6.6	3.2	(*19*)
Raschig rings, clay	Air	12.23	..	0.555	8.3	3.3	(*19*)
	Air	12.23	..	0.622	9.9	2.4	(*19*)
Rhombohedral 3[a]	Water	7.56	..	0.260	2.2	1.4	(*2*)
Orthorhombic 4[a]	Water	7.56	..	0.395	3.4	1.6	(*2*)
Orthorhombic 2, clear	Water	7.56	..	0.395	3.3	1.1	(*2*)
Orthorhombic 2, blocked	Water	7.56	..	0.395	8.7	5.6	(*2*)
Various materials	Different gases	....	..	...	1.7-3.00	2.4-4.5	(*15*)

[a] Configurations and orientations of geometrical packings are described in detail in (*2*).

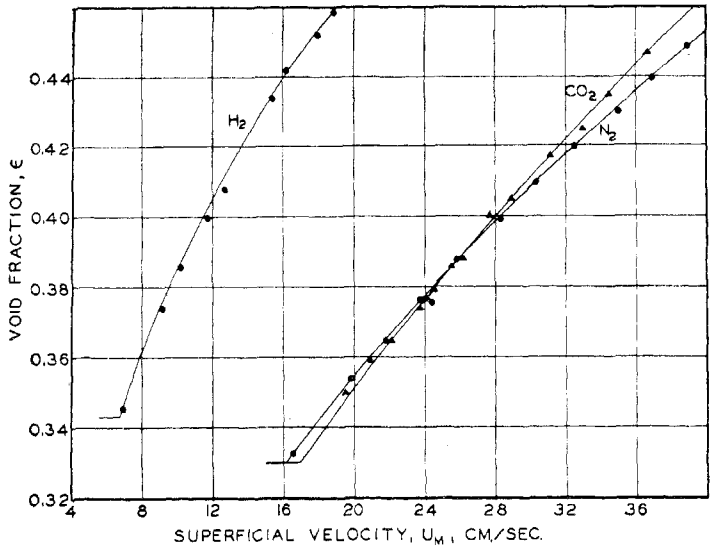

Figure 4. Expansion of Beds of Glass Beads

(Curves drawn according to Equation 12 with break points at ϵ_0)

Gas	Av. Diam. of Spheres, Mm.
H_2	0.227
CO_2	0.570
N_2	0.570

THE EXPANDED BED

When the pressure gradient becomes equal to the buoyant weight of the packing per unit volume of the bed,

$$\frac{dP}{dL} = (1 - \epsilon)(\rho_s - \rho_f)g \qquad (10)$$

the bed begins to expand. Equation 6 remains valid, the pressure gradient being given in Equation 10. The fractional void volume increases with flow rate. Eliminating the pressure gradient between Equations 6 and 10:

$$\epsilon^3 - \frac{2\alpha S_v^2 \mu}{(\rho_s - g)\rho_f}(1 - \epsilon)u = \frac{\beta S_v \rho_f}{8(\rho_s - \rho_f)g} u^2 \qquad (11)$$

gives the fractional void volume in terms of the corresponding velocity, u. This equation is not rigorous as applied to the entire column in terms of u_m, because it neglects the variation in fractional void volume over the length of the bed due to the effect of gas expansion upon velocity. However, this change in ϵ is nearly proportional to the one third power of velocity, and the use of u_m gives a fairly accurate average ϵ over the entire column. A rigorous solution would involve the substitution of appropriate values of u at various lengths L in Equation 11, plotting ϵ *vs.* L, and graphically obtaining the average ϵ over the entire column. This procedure is hardly warranted, for the use of u_m and the over-all fractional void volume yields results well within the limits of experimental accuracy. Therefore, Equation 11 can be written as:

$$\epsilon^3 - \frac{2\alpha S_v^2 \mu}{(\rho_s - \rho_{f_m})g}(1 - \epsilon)u_m = \frac{\beta S_v \rho_{f_m}}{8(\rho_s - \rho_{f_m})g} u_m^2 \qquad (12)$$

Independent knowledge of S_v is not essential. Experimental data for the fixed bed give values of (αS_v^2) and (βS_v). All dependence upon particle size and shape is involved in these quantities. As illustrated in Figures 4 to 6, this relation has been verified experimentally with glass beads, lead shot, and iron shot with various gases. The curves are drawn according to Equation 12, the break points corresponding to ϵ_0, the void fraction of the fixed bed.

For relatively short columns of fine, low density material, the u_m^2 term of Equation 7 can be neglected and Equation 12 can be approximated as:

$$\frac{\epsilon^3}{1 - \epsilon} - \frac{\epsilon_0^3}{1 - \epsilon_0} = \frac{2\alpha S_v^2 \mu}{\rho_s g}(u_m - u_{m_0}) \qquad (13)$$

where the zero subscript designates values at the incidence of expansion. Within the range of fractional void volumes usually encountered, the left-hand member of Equation 13 is nearly proportional to the fractional increase in column height. A constant, c, for the approximate relation

$$\frac{\epsilon^3}{1 - \epsilon} - \frac{\epsilon_0^3}{1 - \epsilon_0} = c\frac{\Delta L}{L_0} \qquad (14)$$

can be chosen such that the calculated values of column height deviate from the true values by not more than 3% in the range from zero to 30% expansion for ϵ_0 greater than 0.35.

This approximation leads to the equation:

$$\Delta L/L_0 = \frac{2\alpha}{c}\frac{S_v^2 \mu}{\rho_s g}(u_m - u_{m_0}) \qquad (15)$$

or for a given bed and fluid

$$\Delta L/L_0 = \text{constant}\,(u_m - u_{m_0}) \qquad (16)$$

Equation 13 can be written more directly as

$$\frac{\epsilon^3}{1 - \epsilon} = \frac{2\,\alpha\, S_v^2 \mu}{\rho_s g} u_m; \quad u_m > u_{m_0} \qquad (17)$$

These equations offer convenient means for determining the expansion of fluidized beds. With a knowledge of the properties of the fluid and the density and specific surface of the material, ϵ

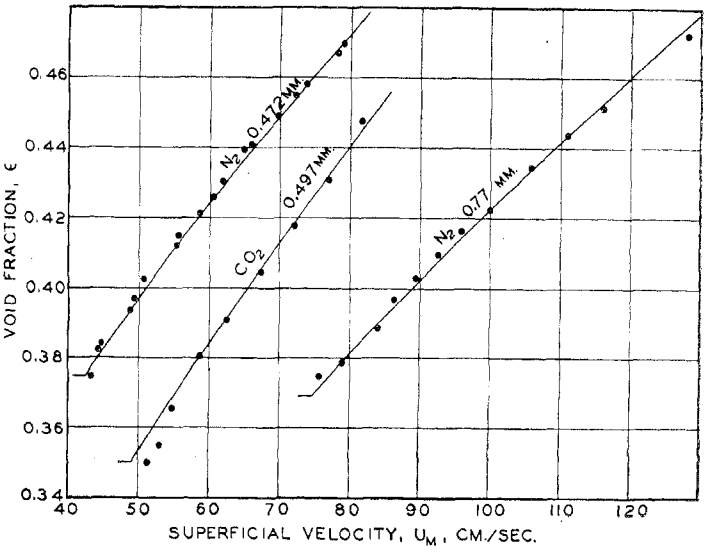

Figure 5. Expansion of Beds of Metal Shot

(Curves drawn according to Equation 12 with break points at ϵ_0)

Material	Gas	Av. Diam. of Spheres, Mm.
Iron	N_2	0.472
Lead	CO_2	0.497
Iron	N_2	0.770

can be obtained from Equation 17 for fluidized systems of fine material of low density. More generally, a single observation of $\Delta L/L_0$ will determine the constant of Equation 16. In the event u_{m_0} cannot be obtained from Equation 12 because of lack of information, another set of values of $\Delta L/L_0$ *vs.* u_m will determine u_{m_0} as well.

Equation 15 has been verified experimentally for pulverized coke and for fine glass beads with various gases. Equation 16 has been found to apply more generally, even when the second term of Equation 7 cannot be neglected, except that the slope must then be determined experimentally and can no longer be predicted from a knowledge of α and β.

THE FLUIDIZED BED

As the gas flow rate is increased, bed expansion continues according to Equation 12. There is a limit, however, to the homogeneous expansion of the bed. At higher flow rates part of the gas flows through a denser but expanded bed which constitutes a continuous phase, while the balance of the gas passes through the bed in bubbles which probably contain solids in suspension. The bubbles constitute a discontinuous phase. The solids are violently agitated and the condition may be termed turbulent or two-phase fluidization. Increasing flow rate causes a larger portion of the gas to flow in the discontinuous phase, approaching a final limit with all the solids in suspension.

With spherical particles, two-phase fluidization was found to begin when the void fraction exceeded a value of about 0.46. This value is nearly that for the void fraction for spheres packed in cubical arrangement, the loosest stable form. This observation suggests that two-phase fluidization does not start before the bed attains the equivalent of the loosest stable configuration. The loosest stable volume was obtained by fluidizing the bed, cutting down the gas flow slowly, and observing the volume when the gas was completely cut off. After the material was packed tightly, gas was let in and the rate of flow increased slowly until two-phase fluidization began. The volume at the start of bubble formation was the same as that obtained by the reverse procedure.

Experiments with closely screened samples of pulverized coke from 16 to 100 mesh gave loosest stable volumes corresponding to void fractions from 0.60 to 0.70 and fractional increase in bed height ranging from 15 to 20%. These estimates for void fraction of coke are arbitrarily based upon a density of 1.4 for the coke which allows for pore volumes not available for fluid flow. The loosest stable packing volumes—i.e., loosest bulk density—for materials having irregular shapes and surface cannot be estimated theoretically, but are easily determined as has been described.

In two-phase fluidization, the denser but expanded phase surrounding the rising bubbles moves towards the bottom of the bed. The rising bubbles carry a portion of the solids to complete the path of circulation. While the solids circulate, there is no substantial circulation of gas.

Because the gas does not flow homogeneously through the bed, contact time and surface effectively contacted are indeterminate. However, for relatively fine solids of low density, the final term of Equation 7 can be neglected and the expansion equation can be used in the form of Equation 17. These equations, for a given bed, depend upon specific gas properties and flow rates only through the product of viscosity times superficial velocity. For this reason, a constant product of viscosity times superficial velocity was chosen as a criterion for a standard state of fluidization for a series of kinetic studies involving gaseous reactions with 60- to 100-mesh coke. With a suitable correction for the partial pressure of the reacting gas component, the resulting rate constants gave a good Arrhenius plot and were directly proportional to the amount of coke in the bed.

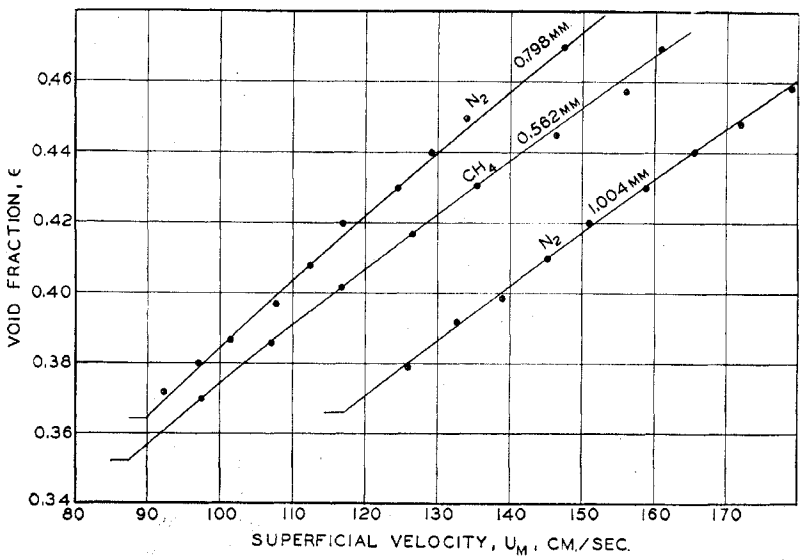

Figure 6. Expansion of Beds of Lead Shot

(Curves drawn according to Equation 12 with break points at ϵ_0)

Gas	Av. Diam. of Spheres, Mm.
N_2	0.798
CH_4	0.562
N_2	1.004

SUMMARY

A general equation has been developed which relates pressure drop to gas flow for fixed beds. The equation shows that the ratio of pressure drop to superficial velocity is a linear function of mass flow rate. Its coefficients depend upon fractional void volume, specific surface of packing material, and fluid viscosity. A transformation of the equation shows that the friction factor implicitly involves the fractional void volume and is not a function of the Reynolds number alone, as has often been assumed.

A fixed bed expands with increasing fluid flow after the pressure drop equals the buoyant weight of the solids per unit area of the bed. The general equation for the fixed bed applies also to the expanding bed; the values of the coefficients remain unchanged. Here the total pressure drop stays constant while the fractional void volume increases. A general form of the equation suitable for calculation of fractional void volume has been given. With suitable approximations equations have been developed which permit direct calculation of such readily observable quantities as fractional expansion or height of the bed. A knowledge of specific surface of the solids is not necessary. Measurement of pressure drop versus flow rate in the fixed bed, employing any gas at a suitable pressure and temperature, is sufficient to determine αS_v^2 and βS_v. The void fraction for the fixed bed, however, must be known.

Expansion is homogeneous until the bed attains the loosest stable configuration of the solids. With gases, additional increase in flow rate causes appearance of bubbles. Under these conditions, the bed is fluidized (two-phase fluidization). The loosest bulk density of any packing material can be determined by fluidizing a sample with a gas in a column and reducing the gas flow slowly. A knowledge of the loosest bulk density is sufficient to estimate flow rates corresponding to the incidence of two-phase fluidization for any gas under any conditions of pressure and temperature.

For kinetic studies of heterogeneous reactions in fluidized beds, a constant product of gas viscosity times superficial velocity may serve as a criterion of a standard state of fluidization—i.e., it will ensure a constant state of fluidization at different temperatures, pressures, and gas compositions. Use of this criterion for a kinetic study of steam and oxygen reactions with coke in fluidized beds, to be reported elsewhere, led to reaction rates that were proportional to the weight of the coke in the bed and gave good Arrhenius plots.

NOMENCLATURE

A = cross-sectional area of column, sq. cm.
c = dimensionless constant
D = diameter of bed, cm.
D_c = diameter of a channel, cm.
D_p = diameter of a spherical particle, cm.
L = length of bed, cm.
N = number of channels per unit area of column
N_{Re} = Reynolds number
ΔP = pressure drop, dynes per sq. cm.
S_t = specific surface, sq. cm. per cc. of solid particle
u^* = average velocity through channel, cm. per second
u = superficial velocity, based on empty tube, cm. per second
u_m = superficial gas velocity at mean of entrance and exit pressures, cm. per second
W = weight rate of fluid flow, grams per second
α = dimensionless coefficient
β = dimensionless coefficient
ϵ = fractional void volume
ρ_f = density of fluid, grams per cc.
ρ_{f_m} = gas density at mean of entrance and exit pressures, grams per cc.
ρ_s = density of solid particles, grams per cc.
μ = viscosity of fluid, poise

LITERATURE CITED

(1) Arnell, J. C., *Can. J. Research*, **24**, A-B, 103 (1946).
(2) Becker, J. C., M.S. thesis, Carnegie Institute of Technology, 1947.
(3) Blake, F. E., *Trans. Am. Inst. Chem. Engrs.*, **14**, 415 (1922).
(4) Brillouin, M., "Leçons sur la viscosité des liquides et des gaz," Paris, Gauthier-Villars, 1907.
(5) Burke, S. P., and Plummer, W. B., IND. ENG. CHEM., **20**, 1196 (1928).
(6) Carman, P. C., *J. Soc. Chem. Ind.*, **57**, 225T (1938).
(7) *Ibid.*, **58**, 1-7T (1939).
(8) Carman, P. C., *Trans. Inst. Chem. Engrs.*, **15**, 150–66 (1937).
(9) Chilton, T. H., and Colburn, A. P., IND. ENG. CHEM., **23**, 913 (1931).
(10) Forchheimer, Ph., "Hydraulik," 3 aufl., p. 54, Leipzig, B. G. Teubner, 1930.
(11) Forchheimer, Ph., *Z. Ver. deut. Ing.*, **45**, 1782 (1901).
(12) Hitchcock, D. I., *J. Gen. Physiol.*, **9**, 755 (1926).
(13) Kozeny, J., *Sitzber. Akad. Wiss. Wien, Math.-naturw. Klasse*, **136** (Abt. IIa), 271–306 (1927).
(14) Lea, F. M., and Nurse, R. W., *J. Soc. Chem. Ind.*, **58**, 277–83T (1939).
(15) Leva, Max, and Grummer, M., *Chem. Eng. Progress*, **43**, 549–54, 633–8, 713–18 (1947).
(16) Lindquist, E., Premier Congrès des Grandes Barrages, Vol. V., pp. 81–99, Stockholm, 1933.
(17) Martin, J., Sc.D. thesis, Carnegie Institute of Technology, 1948.
(18) Muskat, M., "Flow of Homogeneous Fluids through Porous Media," New York, McGraw-Hill Book Co., 1937.
(19) Oman, A. O., and Watson, K. M., *Natl. Petroleum News*, **36**, R795–802 (1944).
(20) Stanton, T. E., and Pannell, J. R., *Trans. Roy Soc. (London)*, (A) **214**, 199–224 (1914).

RECEIVED January 15, 1949.

Flow Characteristics of Solids-Gas Mixtures

In a Horizontal and Vertical Circular Conduit

The isothermal flow characteristics of a solids-gas mixture (alumina, silica, catalyst, and air) are investigated in a horizontal and vertical glass conduit 17 mm. in inside diameter for various rates of air flow and solids flow. Pressure drops across test sections (2.0 feet in length) are accurately measured for a series of air flow rates in which the ratio of solids to air is varied from 0 to 16.0 pounds of solids per pound of air. The solids (catalyst) are introduced into the flow system through a mixing nozzle fed by a slide valve–controlled weighing tank, and have a size distribution varying from particles less than 10 microns to particles greater than 220 microns. Air velocities in the solids-free approach section vary from 50 to 150 feet per second. Several types of nozzles for feeding solids are investigated for stability of flow in the system (absence of pressure surges) and some qualitative information is presented on the type of nozzle yielding the most uniform type of mixing. Qualitative observations on the flow in the solids feed line, mixing nozzle, horizontal and vertical test sections, and short and long radius bends, and the behavior of a multieffect cyclone separator are discussed.

LEONARD FARBAR

UNIVERSITY OF CALIFORNIA, BERKELEY 4, CALIF.

DURING World War II, one of the most remarkable developments in engineering was the application of the continuous flow process to catalytic synthesis. The advantages resulting from a continuous catalytic process—continuous regeneration of catalyst, control of catalyst activity, reaction rate control resulting from the constancy of temperature and thorough mixing in reactors, and finally the economy of long on-stream periods—need not be discussed here. The fluid catalytic units of today offer a most attractive means of carrying out the many Fischer-Tropsch reactions heretofore considered too complex and costly from a commercial point of view.

Although a large number of fluid catalytic crackers have been designed and successfully operated, there appears to be a scarcity of design information in the literature on the hydrodynamic behavior of multicomponent, multiphase systems. This particular field of unit operations has been given some consideration in the past; however, the investigations that have been reported are limited in their application to the fluid units by the fact that studies were limited to particles of fixed and relatively large sizes. Considerable work has been carried out on the investigation of the flow characteristics of gas-liquid mixtures (*1*, *5*, *6*) and a certain amount of attention (*3*, *9*) has been given to the pneumatic conveyance of relatively large solid particles in which the size spectrum was rather limited. Gasterstädt's (*3*) investigation of the transportation of wheat appears to be the first detailed study indicating the possibility that a simple relationship may exist in closed conduits between the pressure drop of a single phase (gaseous) flowing and that encountered when more than one phase is present.